

Electromagnetic Form Factors in the hypercentral CQM

M. De Sanctis¹, M.M. Giannini², E. Santopinto¹, and A. Vassallo¹

¹ Universit a di Genova e INFN, Sezione di Genova, via Dodecaneso 33, 16142 Genova (Italy)

² INFN, Sezione di Roma1, Piazzale Aldo Moro, Roma (Italy)

Received: 05.08.2003 / Revised version: 05.08.2003

Abstract. We report on the recent results of the hypercentral Constituent Quark Model (hCQM). The model contains a spin independent three-quark interaction which is inspired by Lattice QCD calculations and reproduces the average energy values of the $SU(6)$ multiplets. The splittings are obtained with a $SU(6)$ -breaking interaction, which can include also an isospin dependent term. Concerning Constituent Quark models, we have shown for the first time that the decreasing of the ratio of the elastic form factors of the proton is due to relativistic effects using relativistic corrections to the e.m. current and boosts. Now the elastic nucleon form factors have been recalculated, using a relativistic version of the hCQM and a relativistic quark current showing a very detailed reproduction of all the four form factor existing data over the complete range of $0 - 4 \text{ GeV}^2$. Furthermore, the model has been used for predictions concerning the electromagnetic transverse and longitudinal transition form factors giving a good description of the medium Q^2 behaviour. We show that the discrepancies in the reproduction of the helicity amplitudes at low Q^2 are due to pion loops. We have calculated the helicity amplitudes for all the 3 and 4 star resonances opening the possibility of application to the evaluation of cross sections.

PACS. 13.40.Gp Electromagnetic form factors – 12.39.Jh Nonrelativistic quark model – 14.20.Gk Baryon resonances and helicity amplitudes – 12.39.Ki Relativistic quark model – 12.39.Pn Potential Models – 13.40.Gp Electromagnetic Form Factors – 14.30.Gk Baryon Resonances with $S=0$ – 25.20.Lj Photoproduction reactions – 25.30.Rw Electoproduction reactions

1 Introduction

In recent years much attention has been devoted to the description of the internal nucleon structure in terms of constituent quark degrees of freedom. Besides the now classical Isgur-Karl model [1], the Constituent Quark Model has been proposed in quite different approaches: the Capstick and Isgur model [2], the hypercentral formulation [3] and the chiral model [4, 5]. In the following the hypercentral Constituent Quark Model (hCQM), which has been used for a systematic calculation of various baryon properties, will be briefly reviewed. The four electromagnetic elastic form factors of the nucleon have been recently calculated using both a relativistic version of the hCQM and a relativistic current and some results are presented compared with the new data. We have calculated in a systematic way the transverse and longitudinal electromagnetic form factors for all the 3 and 4 star resonances. This effort opens the possibility to many applications for calculations of cross sections (see Ripani contribution for an application to the Jlab two pions data [6]). Finally we will also show how it is possible to reproduce in great detail also the behaviour at low Q^2 of the helicity amplitudes for the nucleon resonances considering chiral corrections to this model (see L. Tiator contribution for more details on pion loop corrections to the hCQM [7]).

2 The hypercentral model

The experimental 4 and 3 star non strange resonances can be arranged in $SU(6)$ -multiplets. This means that the quark dynamics has a dominant $SU(6)$ -invariant part, which accounts for the average multiplet energies. In the hCQM it is assumed to be [3]

$$V(x) = -\frac{\tau}{x} + \alpha x, \quad (1)$$

where x is the hyperradius

$$x = \sqrt{\rho^2 + \lambda^2}, \quad (2)$$

where ρ and λ are the Jacobi coordinates describing the internal quark motion. The dependence of the potential on the hyperangle $\xi = \arctg(\frac{\rho}{\lambda})$ has been neglected.

Interactions of the type linear plus Coulomb-like have been used since long time for the meson sector, e.g. the Cornell potential. This form has been supported by recent Lattice QCD calculations [8].

In the case of baryons a so called hypercentral approximation has been introduced [9, 10], this approximation amounts to average any two-body potential for the three quark system over the hyperangle ξ and works quite well, specially for the lower part of the spectrum [11]. In this respect, the hypercentral potential Eq.1 can be considered as the hypercentral approxima-

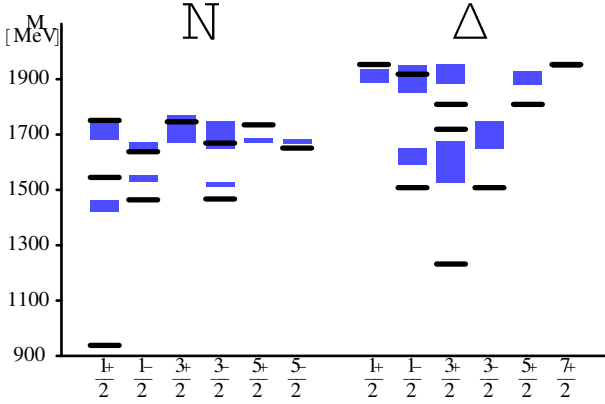


Fig. 1. The spectrum obtained with the hypercentral model Eq.(3) and the parameters Eq. (4) (full lines)), compared with the experimental data of PDG [13] (grey boxes).

tion of the Lattice QCD potential. On the other hand, the hyperradius x is a collective coordinate and therefore the hypercentral potential contains also three-body effects.

The hypercoulomb term $1/x$ has important features [3, 12]: it can be solved analytically and the resulting form factors have a power-law behaviour, at variance with the widely used harmonic oscillator; moreover, the negative parity states are exactly degenerate with the first positive parity excitation, providing a good starting point for the description of the spectrum.

The splittings within the multiplets are produced by a perturbative term breaking the $SU(6)$ symmetry, which, as a first approximation, can be assumed to be the standard hyperfine interaction H_{hyp} [1]. The three quark hamiltonian for the hCQM is then:

$$H = \frac{p_\lambda^2}{2m} + \frac{p_\rho^2}{2m} - \frac{\tau}{x} + \alpha x + H_{hyp}, \quad (3)$$

where m is the quark mass (taken equal to $1/3$ of the nucleon mass). The strength of the hyperfine interaction is determined in order to reproduce the $\Delta - N$ mass difference, the remaining two free parameters are fitted to the spectrum, reported in Fig.1, leading to the following values:

$$\alpha = 1.61 \text{ fm}^{-2}, \quad \tau = 4.59. \quad (4)$$

Keeping these parameters fixed, the model has been applied to calculate various physical quantities of interest: the photocouplings [14], the electromagnetic transition amplitudes [15], the elastic nucleon form factors [16] and the ratio between the electric and magnetic proton form factors [17]. Some results of such parameter free calculations are presented in the next section.

3 The results

The electromagnetic transition amplitudes are defined as the matrix elements of the electromagnetic interaction, between the

nucleon, N , and the resonance, B , states:

$$\begin{aligned} A_{1/2} &= \langle B, J', J'_z = \frac{1}{2} | H_{em}^t | N, J = \frac{1}{2}, J_z = -\frac{1}{2} \rangle \zeta \\ A_{3/2} &= \langle B, J', J'_z = \frac{3}{2} | H_{em}^t | N, J = \frac{1}{2}, J_z = \frac{1}{2} \rangle \zeta \\ S_{1/2} &= \langle B, J', J'_z = \frac{1}{2} | H_{em}^l | N, J = \frac{1}{2}, J_z = \frac{1}{2} \rangle \zeta \end{aligned} \quad (5)$$

where ζ is the sign of the $N\pi$ amplitude.

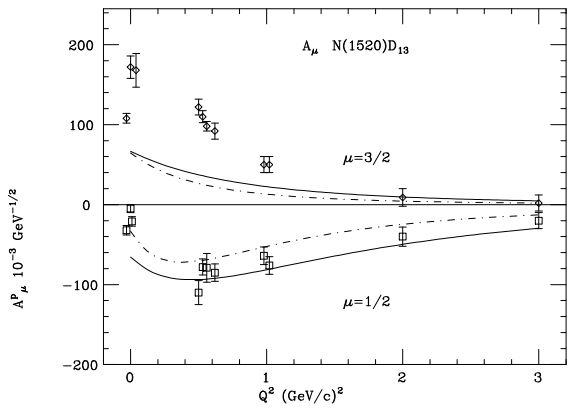


Fig. 2. The helicity amplitudes for the $D_{13}(1520)$ resonance, calculated with the hCQM of Eqs. (3) and (4) (full curve, [15]). The dashed curve is obtained with the analytical version of the hCQM ([12]), where the behaviour of the quark wave function is determined mainly by the hypercoulomb potential. The data are from the compilation of ref. [21]

The proton photocouplings of the hCQM [14] (Eq. (5) calculated at the photon point), in comparison with other calculations [19, 24], have the same overall behaviour, having the same $SU(6)$ structure in common, but in many cases they all show a lack of strength.

Taking into account the Q^2 behaviour of the transition matrix elements of Eq. (5), one can calculate the hCQM helicity amplitudes in the Breit frame [15]. The hCQM results for the $D_{13}(1520)$ and the $S_{11}(1535)$ resonances [15] are given in Fig.2 and 3, respectively. The agreement in the case of the S_{11} is remarkable, the more so since the hCQM curve has been published three years in advance with respect to the recent TJNAF data [22]. We have completed our program in order to calculate in a systematic way the helicity amplitudes, transverse and longitudinal ones, for all the 3 and 4 star resonances (the results are at disposal under request) [23]. In general the Q^2 behaviour is reproduced, except for discrepancies at small Q^2 , especially in the $A_{3/2}^p$ amplitude of the transition to the $D_{13}(1520)$ state. These discrepancies, as the ones observed in the photocouplings, can be ascribed either to the non-relativistic character of the model or to the lack of explicit quark-antiquark configurations, which may be important at low Q^2 . The kinematical relativistic corrections at the level of boosting the nucleon and the resonance states to a common frame are not responsible for

these discrepancies, as we have demonstrated in Ref. [26]. Similar results are obtained for the other negative parity resonances [15].

It should be mentioned that the r.m.s. radius of the proton corresponding to the parameters of Eq. (4) is 0.48 fm, which is the same value obtained in [18] in order to reproduce the D_{13} photocoupling. Therefore the missing strength at low Q^2 can be ascribed to the lack of quark-antiquark effects, probably more important in the outer region of the nucleon.

For example, for the Delta resonance the contribution of the pion cloud is very important [7]. For the transverse amplitudes $A_{1/2}$ and $A_{3/2}$ it is about 50% at low Q^2 and for the longitudinal amplitude as well as for the electric amplitude the pion cloud is absolutely dominant.

In Fig. 4 we show for the $A_{3/2}$ amplitude that only the sum of both contribution will get close to the empirical results.

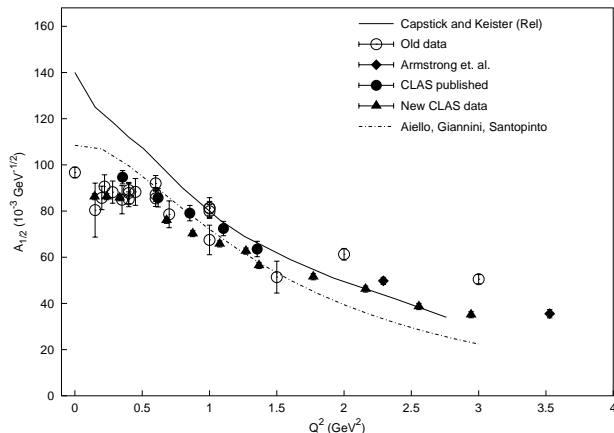


Fig. 3. The helicity amplitudes for the $S_{11}(1535)$ resonance, calculated with the hCQM of Eqs. (3) and (4) (dotted curve, [15]) and the model of ref. [24] (full curve). The data are taken from the compilation of ref. [25]

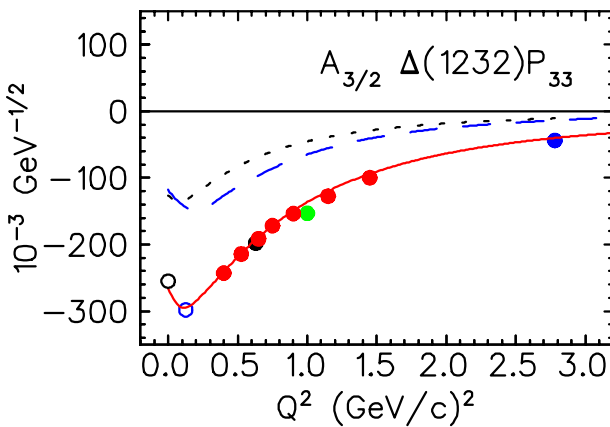


Fig. 4. The transverse $A_{3/2}$ helicity amplitude for the $\Delta(1232)$ resonance. The dotted line corresponds to the hCQM results, the dashed line to the pion loop contributions and the full line to a fit of the existing data (see L.Tiator contribution for a complete explanation).

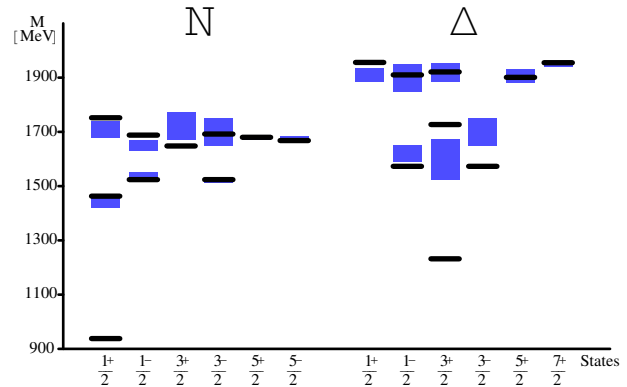


Fig. 5. The spectrum obtained with the hypercentral model containing isospin dependent terms Eq. (7) [27] (full lines), compared with the experimental data of PDG [13] (grey boxes)

4 The isospin dependence

In the chiral Constituent Quark Model [4,5], the non confining part of the potential is provided by the interaction with the Goldstone bosons, giving rise to a spin- and flavour-dependent part, which is crucial in this approach for the description of the lower part of the spectrum. More generally, one can expect that the quark-antiquark pair production can lead to an effective residual quark interaction containing an isospin (flavour) dependent term. Therefore, we have introduced isospin dependent terms in the hCQM hamiltonian. The complete interaction used is given by [27]

$$H_{int} = V(x) + H_S + H_I + H_{SI}, \quad (6)$$

where $V(x)$ is the linear plus hypercoulomb SU(6)-invariant potential of Eq. 1, while the remaining terms are the residual SU(6)-breaking interaction, responsible for the splittings within the multiplets. H_S is a smeared standard hyperfine term, H_I is isospin dependent and H_{SI} spin-isospin dependent. The resulting spectrum for the 3 and 4 star resonances is shown in Fig. 5 [27]. The contribution of the hyperfine interaction to the $N - \Delta$ mass difference is in this case only about 35%, while the remaining splitting comes from the spin-isospin term, (50%), and from the isospin one, (15%). It should be noted that the position of the Roper and the negative parity states is well reproduced.

5 Relativity

The relativistic effects that one can introduce starting from a non relativistic quark model are: a) the relativistic kinetic energy; b) the boosts from the rest frames of the initial and final baryon to a common (say the Breit) frame; c) a relativistic quark current. All these features are not equivalent to a fully relativistic dynamics, which is still beyond the present capabilities of the various models.

The potential of Eq.1 has been refitted using the correct relativistic kinetic energy

$$H_{rel} = \sum_{i=1}^3 \sqrt{p_i^2 + m^2} - \frac{\tau}{x} + \alpha x + H_{hyp}. \quad (7)$$

The resulting spectrum is not much different from the non relativistic one and the parameters of the potential are only slightly modified.

The boosts and a relativistic quark current expanded up to lowest order in the quark momenta has been used both for the elastic form factors of the nucleon [16] and the helicity amplitudes [26]. In the latter case, as already mentioned, the relativistic effects are quite small and do not alter the agreement with data discussed previously. For the elastic form factors, the relativistic effects are quite strong and bring the theoretical curves much closer to the data; in any case they are responsible for the decrease of the ratio between the electric and magnetic proton form factors, as it has been shown for the first time in Ref. [17], in qualitative agreement with the recent Jlab data [28].

A relativistic quark current, with no expansion in the quark momenta, and the boosts to the Breit frame have been applied to the calculation of the elastic form factors in the relativistic version of the hCQM Eq. (7) [29]. The resulting theoretical form factors of the proton, calculated, it should be stressed, without free parameters and assuming pointlike quarks, are good with some discrepancies at low Q^2 , which, as discussed previously, can be attributed to the lacking of the quark-antiquark pair effects. Concerning the ratio between the electric and magnetic proton form factors the deviation from unity reaches almost the 50% level, not far from the new TJNAF data [30]. Nevertheless to obtain a full description of the existing data on

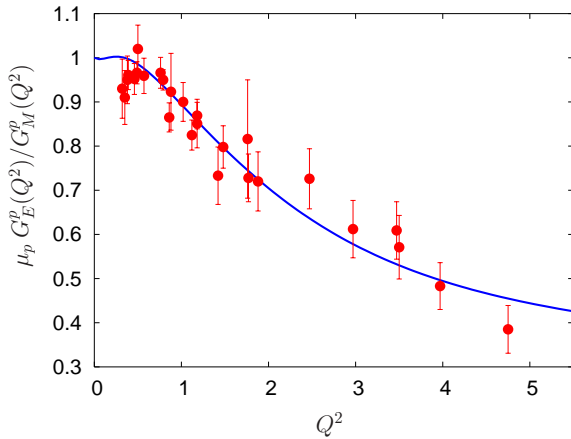


Fig. 6. The ratio between the electric and magnetic proton form factors, calculated with the relativistic hCQM of eq. (8), a relativistic current and a small constituent quark form factor [29], compared with the TJNAF data [28, 30]

the elastic form factors one still has to take into account the $q\bar{q}$ degrees of freedom. A way to describe effectively the effect of these extra degrees of freedom is to introduce constituent quark form factors. Adding the effect of small constituent quark form factor to the hCQM results, the curve shown in Fig. 6 is obtained.

6 Conclusions

The hCQM is a generalization to the baryon sector of the widely used quark-antiquark potential containing a coulomb plus a lin-

ear confining term. The three free parameters have been adjusted to fit the spectrum [3] and then the model has been used for a systematic calculation of various physical quantities: the photocouplings [14], the helicity amplitudes for the electromagnetic excitation of negative parity baryon resonances [15, 26, 23], the elastic form factors of the nucleon [16, 29] and the ratio between the electric and magnetic proton form factors [17, 29]. The agreement with data is quite good, specially for the helicity amplitudes, which are reproduced in the medium-high Q^2 behaviour, leaving some discrepancies at low (or zero) Q^2 , where the lacking quark-antiquark contributions are expected to be effective. It should be noted that the hypercoulomb term in the potential is the main responsible of such an agreement [12], while for the spectrum a further fundamental aspect is provided by the isospin dependent interactions [27]. We have completed our program calculating the transverse and longitudinal helicity amplitudes for all the resonances [23], opening in this way the possibility of applications to the calculation of cross sections, as for example in the two pion case [6] (see Fig. 7). Finally, we have calculated the chiral corrections to our helicity amplitudes showing an impressive reproduction of all the existing data [7].

References

1. N. Isgur and G. Karl, Phys. Rev. **D18**, 4187 (1978); **D19**, 2653 (1979); **D20**, 1191 (1979); S. Godfrey and N. Isgur, Phys. Rev. **D32**, 189 (1985)
2. S. Capstick and N. Isgur, Phys. Rev. **D 34**, 2809 (1986)
3. M. Ferraris, M.M. Giannini, M. Pizzo, E. Santopinto and L. Tiator, Phys. Lett. **B364**, 231 (1995); E. Santopinto, PhD Thesis, Università di Genova (1995).
4. L. Ya. Glozman and D.O. Riska, Phys. Rep. **C268**, 263 (1996).
5. L. Ya. Glozman, Z. Papp, W. Plessas, K. Varga and R. F. Wagenbrunn, Phys. Rev. **C57**, 3406 (1998); L. Ya. Glozman, W. Plessas, K. Varga and R. F. Wagenbrunn, Phys. Rev. **D58**, 094030 (1998).
6. M. Ripani, to be published on Eur.Phys.J.(2004)
7. L. Tiator, D. Drechsel, S. Kamalov, E. Santopinto, M.M. Giannini, A. Vassallo to be published on Eur.Phys.J. (2004)
8. G. Bali et al., Phys. Rev. **D51**, 5165 (1995); G. Bali, Phys. Rept. **343**, 1 (2001)
9. P. Hasenfratz, R.R. Horgan, J. Kuti and J.M. Richard, Phys. Lett. **B94**, 401 (1980)
10. J.-M. Richard, Phys. Rep. **C 212**, 1 (1992)
11. M. Fabre de la Ripelle and J. Navarro, Ann. Phys. (N.Y.) **123**, 185 (1979).
12. E. Santopinto, F. Iachello and M.M. Giannini, Nucl. Phys. **A623**, 100c (1997); Eur. Phys. J. **A1**, 307 (1998)
13. Particle Data Group, Eur. Phys. J. **C15**, 1 (2000).
14. M. Aiello, M. Ferraris, M.M. Giannini, M. Pizzo and E. Santopinto, Phys. Lett. **B387**, 215 (1996).
15. M. Aiello, M. M. Giannini and E. Santopinto, J. Phys. G: Nucl. Part. Phys. **24**, 753 (1998)
16. M. De Sanctis, E. Santopinto and M.M. Giannini, Eur. Phys. J. **A1**, 187 (1998).
17. M. De Sanctis, M.M. Giannini, L. Repetto and E. Santopinto, Phys. Rev. **C62**, 025208 (2000).
18. L. A. Copley, G. Karl and E. Obryk, Phys. Lett. **29**, 117 (1969).
19. R. Koniuk and N. Isgur, Phys. Rev. **D21**, 1868 (1980).
20. F. E. Close and Z. Li, Phys. Rev. **D42**, 2194 (1990); Z. Li and F.E. Close, Phys. Rev. **bf D42**, 2207 (1990).

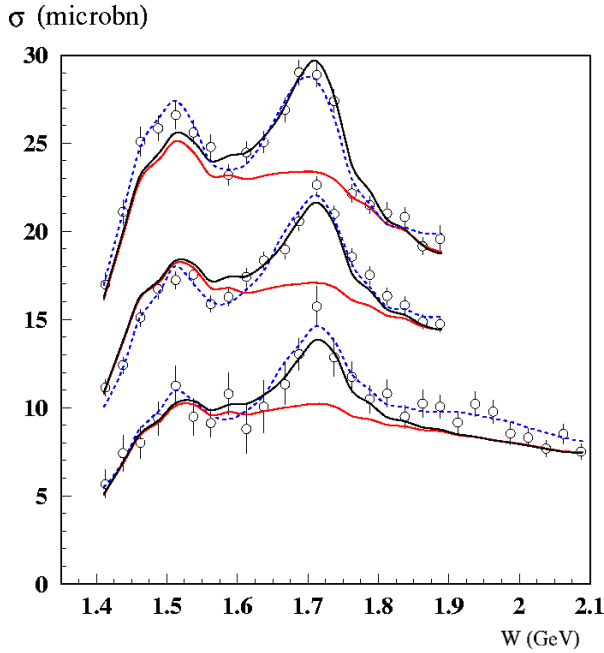


Fig. 7. Comparison of the new CLAS data for the two pion total cross section with the calculation based on the electromagnetic helicity amplitudes from the hCQM, transverse and longitudinal ones, the solid line is the result obtained including also the new state found by their previous analysis. The explanation of this picture and of the work can be found on Ripani's contribution.

21. V. D. Burkert, private communication
22. R.A. Thompson et al., Phys. Rev. Lett. **86**, 1702 (2001).
23. M. M. Giannini, E. Santopinto, A. Vassallo, to be published.
24. S. Capstick and B.D. Keister, Phys. Rev. **D 51**, 3598 (1995)
25. V. D. Burkert, arXiv:hep-ph/0207149.
26. M. De Sanctis, E. Santopinto and M.M. Giannini, Eur. Phys. J. **A2**, 403 (1998).
27. M.M. Giannini, E. Santopinto and A. Vassallo, Eur. Phys. J. **A12**, 447 (2001).
28. M.K. Jones et al., Phys. Rev. Lett. **B84**, 1398 (2000).
29. M. De Sanctis, M.M. Giannini, E. Santopinto and A. Vassallo, to be published.
30. O. Gayon et al., Phys. Rev. Lett. **88**, 092301 (2002).
31. M.M. Giannini, E. Santopinto, A. Vassallo, M. De Sanctis, to be published on Eur.Phys.J. (2004)